A Ka-BAND HIGH-EFFICIENCY DIELECTRIC LENS ANTENNA WITH A SILICON MICROMACHINED MICROSTRIP PATCH RADIATOR

Ushio Sangawa, Kazuaki Takahashi, Takeharu Urabe*, Hiroshi Ogura* and Hiroyuki Yabuki

Matsushita Research Institute Tokyo, Inc.
*Matsushita Electric Ind. Co, Ltd.
3-10-1 Higashimita, Tama-ku Kawasaki, 214-8501, Japan

Abstract — **Novel antenna configurations suitable for millimeter-wave applications were proposed incorporating a dielectric lens antenna with a single microstrip patch radiator. In general high aperture efficiencies are easily obtainable with lens antennas because of flexibility in controlling the aperture-field distribution coupled with low feeder loss. The radiator was integrated with front-end circuits into a single hybrid IC using silicon micromachining and BCB (benzocyclobutene) multi-stacked circuit processes. The radiator was constructed on a thin suspended BCB film to suppress dielectric and conductor loss. A demonstration radiator showed good performance at 39 GHz (Ka-band). The lens was designed using geometrical optics relative to the directivity of the radiator and the aperture-field distribution. The circular polarized lens antenna assembly exhibited a gain of 15.7 dBi, 18.7 dB side-lobe level suppression and 0.17 dB axial ratio.**

I. INTRODUCTION

Currently, use of commercial millimeter-wave applications is rapidly growing in modern high-speed wireless access systems. For these applications, antennas with a gain of about 15 dBi~30 dBi are required. In general, system designs incorporate aperture antennas with waveguide based signal ports. However, this configuration has problems in interconnection with circuits and its large volume. From the point of the antenna configuration, array antennas composed of microstrip circuits seem to be adequate, but they display poor radiation efficiency because of serious feeder losses. To overcome these difficulties, various efforts have been investigated including the integration of array antennas into a front end IC with other circuit [1][2], application of a low loss line structure and new fabrication technology [3][4] and so on.

In this paper, in order to resolve difficulties related to interconnection and feeder loss, we propose a dielectric lens antenna configuration. In addition, in order to obtain a much higher radiation efficiency, we adopted a micromachined microstrip patch antenna (MSA) with a low loss line structure as the radiator. We discuss the designing considerations of lens antennas based on geometrical optics and the properties of micromachined patch radiator in detail. Results of a fabricated antenna at 39 GHz are also demonstrated.

II. CONFIGURATION OF PROPOSED ANTENNA

Fig. 1 shows the conceptual structure of the proposed dielectric lens antenna. A radiator was integrated with the millimeter-wave front-end circuits into a single hybrid IC (HIC) on silicon substrate. In addition to the compact circuit configuration, no mechanical interconnection part is required between the circuit and the aperture. Consequently, minimized feeder and interconnection losses together with a high radiation efficiency are expected.

Lens antennas display the following two advantages. One is easy control of the aperture-field distribution allowing low sidelobe and the high aperture efficiency to be easily obtainable. The second is that the redesign of the HIC to fit applications is unnecessary because the directivity of the lens antenna is determined by the aperture-field distribution and aperture size alone.

Despite these advantages, availability of a dielectric material displaying low dielectric loss in millimeter-wave band and suited fabrication characteristics remains elusive.

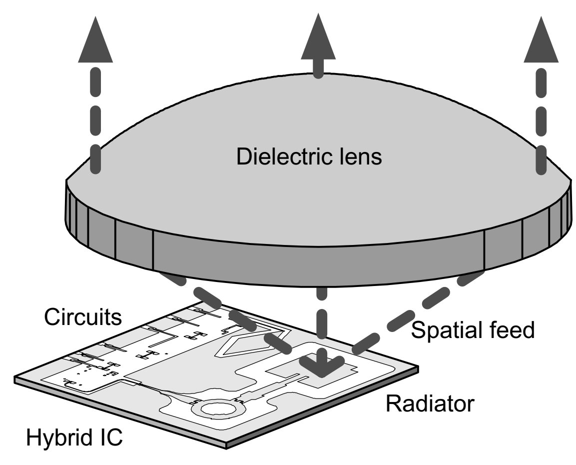

Fig. 1. Conceptual structure of the proposed antenna.

However, recently we have been able to select a number of materials in addition to Teflon, and a solution to this difficulty.

III. Lens Antenna Designing Methodology

A crucial step is the determination of the two refractive surfaces of the lens. We applied geometrical optics fully justified such that the wavelength is negligibly shorter than the aperture size. With this method, the two curvatures of the lens are determined as numerical solutions using the following four equations (1)~(4) when the directivity of the radiator and the aperture-field distributions are known. Definitions of symbol and coordinates representing the curvatures of the lens are shown in Fig. 2. Equation (1) and (2) denote the Snell's law for curvature 1 and 2 respectively. Equation (3) sets the same optical length for all paths, and guarantees the absence of aberration on the optical axis and free of phase error on the aperture plane. The last equation states the law of the energy conservation. Here, we use the Runge-Kutta method for solving these equations numerically.

$$\frac{dr}{d\theta} = r\frac{n\sin(\theta-\varphi)}{n\cos(\theta-\varphi)-1} \tag{1}$$

$$\frac{dz}{d\theta} = \frac{n\sin\varphi}{1-n\cos\varphi}\frac{dx}{d\theta} \tag{2}$$

$$r + n\frac{z_0 - r\cos\theta}{\cos\varphi} + (z_0 - z) = const. \tag{3}$$

$$\frac{dx}{d\theta} = \frac{|E_p(\theta)|^2 \sin\theta \int_0^{x\max} dx\, x\, |E_d(x)|^2}{|E_d(x)|^2\, x \int_0^{\theta\max} d\theta \sin\theta\, |E_p(\theta)|^2} \tag{4}$$

A lens was designed to yield a sidelobe level of less than - 20dB and the gain is about 15 dBi. The aperture diameter and the aperture-field distribution were then

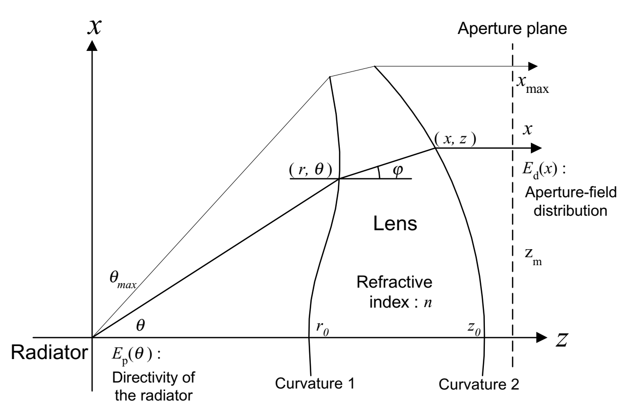

Fig. 2. Definitions of symbols and coordinates representing lens curvatures and design equations.

TABLE I
Aperture Performances

Aparture diameter	40 mm (5.1 λ)
Aparture-field distribution	- 30 dB Taylor (n = 3) $E_d(x) \propto \frac{2}{\pi^2} + \sum_{m=1}^{n-1} g_m J_0(\lambda_m x)$ $g_1 = 0.201158$ $g_2 = -0.001334$

determined as shown in table I. The aperture size was calculated from the required gain and the field distribution was designed taking the sidelobe level, the aperture efficiency and the simplified field distribution into consideration.

We adopt polyetherimide resin composite material from the viewpoint of the fabrication as the dielectric material. Upon solving these equations, it is important to notice that they do not gives a unique lens shape but yield many sets of curvature. Then it is necessary to choose one solution from these from which it is necessary to select one as the solution. As a consequence, we imposed additional conditions that minimized spill over, minimized the reflection angles at each curvatures to prevent the reflection, and shortened the focal length for a compact antenna configuration.

The lens was fabricated by numerical controlled lathe. Generally in optics, the phase difference from the aberration-free ideal wavefront should be less than 1/8~1/16 λ in terms of propagating wavelength in order to show sufficient optical performance. The necessary calculated surface accuracy was required to be less than 270 μm, an error easily within the parameter of the lathe.

IV. Configuration of the Radiator

The radiator has a microstrip line structure on a freely suspended BCB thin film, as shown in Fig. 3. The structure is fabricated by photolithography and silicon micro-

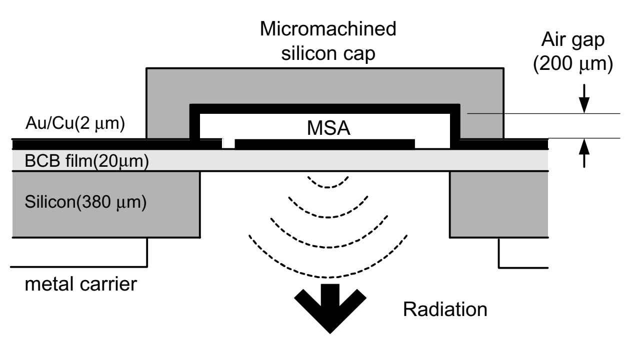

Fig. 3. Cross-sectional view of the layer structure. The radiator is located on the freely suspended BCB film.

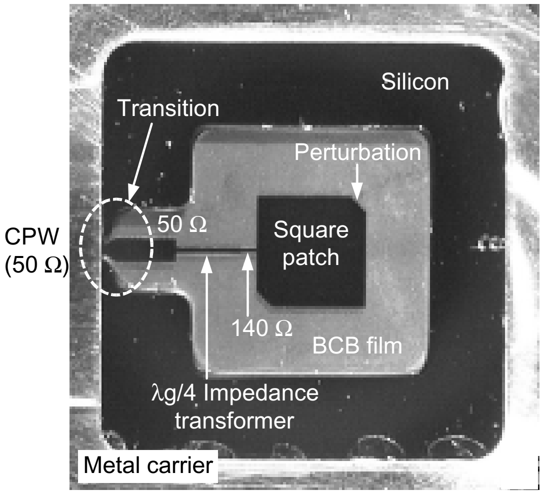

Fig. 4. Top view of the fabricated radiator.

machining technology. Firstly, all of the circuits are patterned onto a 20 µm BCB film. Next the 380 µm thick silicon substrate is perfectly removed from the backside of the substrate by using dry-etching technology, leaving the BCB film only remained. The last step, a metallic silicon cap with 200 µm deep hollows is bonded to the chip by soldering. The cap is also fabricated by the same processes as the radiator. Au/Cu (2 µm) metal layers are stacked on the BCB. We adopted this structure in order to increase radiation efficiency. This time, by applying BCB as a supporting dielectric, sufficient mechanical strength and simplified processes could be realized.

The antenna applied as the radiator is configured as a single fed square MSA. The radiator was circular-polarized by adding small perturbations to opposing diagonal corners of the patch for splitting two degenerate modes as shown in Fig. 4. The feed point could be located at the edge of the patch, allowing the current distribution in the MSA to remain is undisturbed. Thus a good axial ratio is expected with the addition of no other structural correction. The reason for this feeding structure is explained in its structure shown in Fig. 3. The smaller the dielectric constant in the substrate, the smaller the input impedance of MSA becomes. This makes it easy to connect a 50 Ω line to the feed point merely by inserting an impedance transformer. Finally we should mention that the transition is added at the feed port to allow investigation of properties when it will be connected to other circuits with the BCB multi-stacked structure.

V. Results

A. Properties of fabricated Radiator

To begin with, we have investigated properties of the radiator only. Frequency dependency of the matching properties at the input port (CPW port shown in the Fig. 3) is shown in Fig. 5. Good agreements with designed values can be seen. The bandwidth where the VSWR is less than 2 is 2.6 GHz (relative bandwidth 6.7 %), and showed a much wider response than the conventional MSA on a typical dielectric, such as Teflon. This is due to the low effective dielectric constant of this layer structure.

The measured directivity and other radiation performance parameters at the resonant frequency of 39 GHz are shown in Fig. 6. From the directivity, the half-power beamwidth was 56 degree, and slightly narrower than the theoretical value. This is thought to be due to the inter-

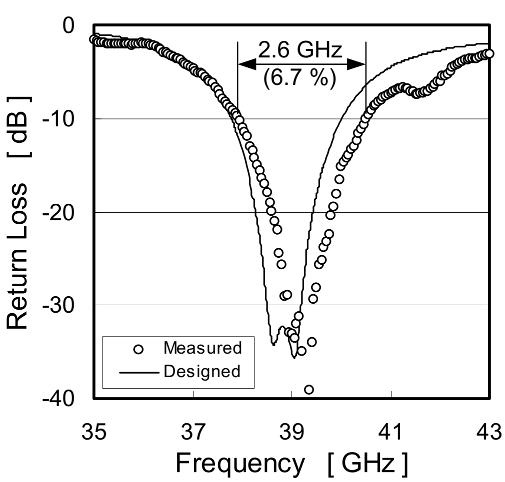

Fig. 5. Measured and calculated frequency response of the radiator.

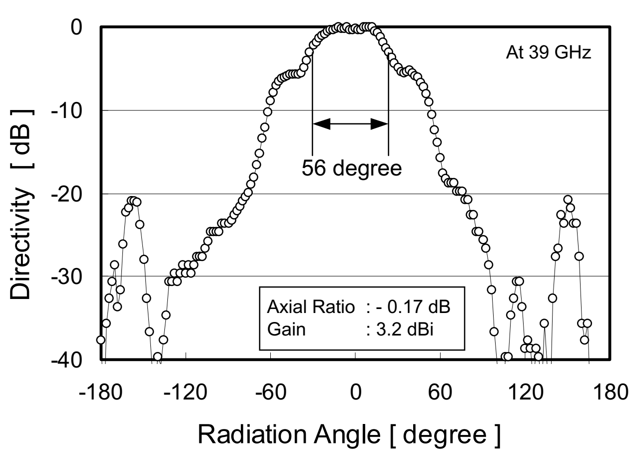

Fig. 6. Measured radiation properties of the fabricated radiator.

ference between the main beam and the diffraction wave components that are generated at pattern edges adjacent to the MSA.

The gain and axial ratio were measured by comparing with standard gain horn antennas. Although the feeding loss is included in the measured values, a gain of 3.2 dBi shows that a high radiation efficiency could be obtained. The resultant axial ratio of 0.17 dB gives credence to discussions mentioned above.

B. Overall Performance

We show the photograph of the assembled antenna in Fig. 7. Whole size is 50 mm x 50 mm x 36 mm. The compactness is achieved. Overall radiation performance is shown as in Fig. 8. The measured gain of 15.3 dBi is in good agreement with a designed value 15.7 dBi, realizing a high aperture efficiency of 73 %. Good polarization property is also observed, and it is confirmed that there is no degeneration caused by attaching the lens. Sidelobe level appears to be degraded, and is considered to be due to influence of the inner shape of the antenna body and the diffraction phenomena. This can be improved by using other electromagnetic analysis, such as finite difference time domain method or finite element method.

VI. CONCLUSIONS

We proposed a dielectric lens antenna with a microstrip radiator as a candidate for millimeter-wave communication systems and fabricated a Ka-band antenna using silicon micromachining technology. We have successfully designed a 39 GHz lens antenna incorporating geometrical optics. The antenna has showed good radiation properties as a result of adopting a low loss line structure in addition to characteristic properties typical of lens antennas. It was confirmed that this antenna configuration could be easily applied to various higher band millimeter-wave applications such as a 60 GHz radio-link.

ACKNOWLEDGEMENT

The authors wish to acknowledge the assistance and support of Dr. M Makimoto, K. Nagao and Telecommunications Advancement Organization of Japan (TAO).

REFERENCES

[1] S. Fujita, U. Sangawa, K. Takahashi, K. Goho, S. Takeyama, H. Ogura, and H. Yabuki, "Millimeter-wave Transceiver MCM Using Multi-layer BCB with Integrated Planer Antenna," *in 29 th European Microwave Conference'99 Dig.*, vol. Vol. 1, pp. 91-94, Oct. 1999.

[2] M. Singer, K. M. Strohm, J. –F. Luy, and E. M. Biebl, "Active SIMMWIC-antenna for automotive applications," *in 1997 IEEE MTT-S Int. Microwave Symp. Dig. (Denver, Col.)*, pp. 1265-1268, June 1997.

[3] S. V. Robertson, L. P. B. Katehi, and G. M. Rebeiz, "Micromachined W-Band Filters," *IEEE Trans. Microwave Theory Tech.*, vol. 44, no. 4, pp. 598-606, Apr. 1996.

[4] U. Sangawa, S. Fujita, K. Takahashi, A. Ono, H. Ogura, and H. Yabuki, "Micromachined Millimeter-Wave Devices with Three Dimensional Structure," *in 1998 Asia-Pacific Microwave Conference Dig.*, vol. 2, pp. 505-508, Dec. 1998.

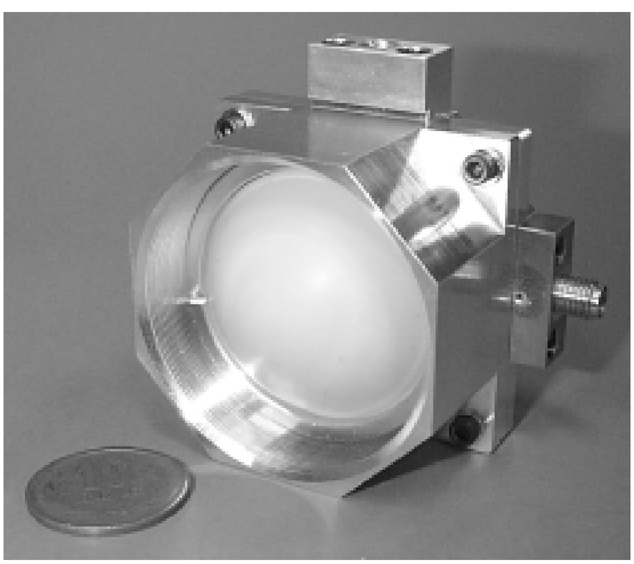

Fig. 7. Photograph of the assembled antenna. A 10-yen coin (23.5 mm in diameter) is for comparison.

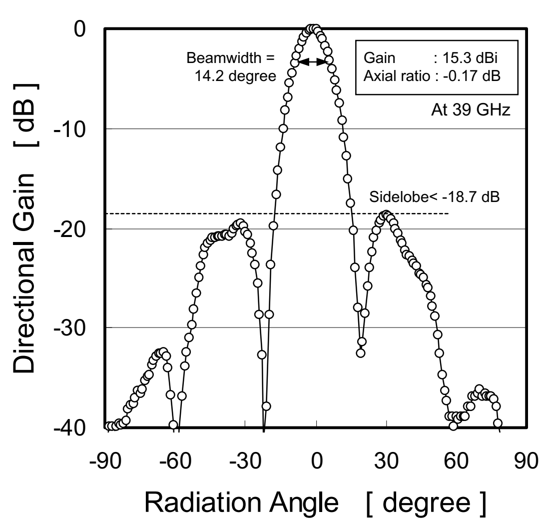

Fig. 8. Radiation properties of the demonstrated lens antenna .